

ROSE: A Recognition-Oriented Speech Enhancement Framework in Air Traffic Control Using Multi-Objective Learning

Xincheng Yu¹, Dongyue Guo¹, Jianwei Zhang¹, Yi Lin^{1*}

¹College of Computer Science, Sichuan University, Chengdu, China
yuxincheng1998, dongyueguo@stu.scu.edu.cn
zhangjianwei, yilin@scu.edu.cn

Abstract

Radio speech echo is a specific phenomenon in the air traffic control (ATC) domain, which degrades speech quality and further impacts automatic speech recognition (ASR) accuracy. In this work, a recognition-oriented speech enhancement (ROSE) framework is proposed to improve speech intelligibility and also advance ASR accuracy, which serves as a plug-and-play tool in ATC scenarios and does not require additional retraining of the ASR model. Specifically, an encoder-decoder-based U-Net framework is proposed to eliminate the radio speech echo based on the real-world collected corpus. By incorporating the SE-oriented and ASR-oriented loss, ROSE is implemented in a multi-objective manner by learning shared representations across the two optimization objectives. An attention-based skip-fusion (ABSF) mechanism is applied to skip connections to refine the features. A channel and sequence attention (CSAtt) block is innovatively designed to guide the model to focus on informative representations and suppress disturbing features. The experimental results show that the ROSE significantly outperforms other state-of-the-art methods for both the SE and ASR tasks. In addition, the proposed approach can contribute to the desired performance improvements on public datasets.

Introduction

In air traffic control (ATC), speech is a primary means to achieve air-ground communication between the air traffic controller (ATCO) and the aircrew. ATCO issues spoken ATC instructions via the very high frequency radio to provide required services for aircrew, whereas the aircrew reads back the received instructions promptly to ensure a consentient understanding of the flight operation. In this procedure, the automatic speech recognition (ASR) technique is a preferred solution to convert the spoken instruction into readable texts, based on which contextual ATC elements are extracted to obtain traffic dynamics and further support ATC operations (Oualil et al. 2017; Lin et al. 2021c).

Recently, enormous efforts have been made to achieve the ASR task (Badrinath and Balakrishnan 2022; Lin et al. 2021b,a). By analyzing the ASR results, volatile noise is a major issue to limit ASR performance in the ATC environment, referring to the environment noise, device noise, radio transmission noise, speech echo, etc. Unlike the additive

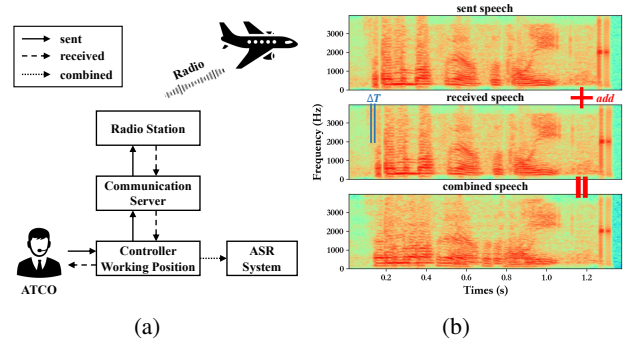


Figure 1: (a) The mechanism of the ATC speech transmission. (b) The speech spectrograms of different procedures generated by the CWP.

non-stationary signal (i.e., environment, device, radio), the speech echo is a specific overlapping phenomenon dedicatedly generated by the ATC communication between the sent and received ATCO speech.

As shown in Figure 1 (a), the spoken instructions issued by ATCO are passed to the controller working position (CWP), the communication server, and finally to the radio stations, which are further forwarded to the aircrew (sent speeches). To ensure that the issued ATCO spoken instructions can be successfully received by receivers, based on the ATC procedure, the sent ATCO instructions are also returned to the assistant ATCO of the corresponding CWP to allow the ATCO to confirm the communication reliability (received speeches). Finally, the combined speeches are determined by addition operation based on the sent and received speeches in the CWP and fed into the following ASR systems, which can provide an integrated speech interface and reduce the system complexity.

Due to the returned ATCO instructions, a temporal delay between the sent speech and the received speech exists in the combined speech, which is defined as *speech echo*. As shown in Figure 1 (b), the speeches (only from ATCO) collected from CWP are outlined in the spectrogram manners and the time offset (ΔT) is presented in the received speech. Compared to uncombined signals (sent or received speech), the combined speech spectrogram is distorted by redundant

*Corresponding author.

echo interference of signal overlapping, which further degrades the perception and intelligibility of the ATCO speech. By investigating the ASR performance, the accuracy of the ATCO speech (with speech echo) is obviously lower than that of the aircrew speech (without speech echo). Therefore, compared to other additive non-stationary noises, due to the ATC specificities, it is believed that the ASR performance can be significantly advanced by tackling the speech echo to enhance the speech quality.

Since the temporal delay is affected by many factors (distance between CWP and radio station, radio frequency, etc.), the value of ΔT is varied between 10 and 200 milliseconds, which is distinct for each utterance. Therefore, the redundant effect of speech echo is considered as special coupling noise and is not the solo reverberation or echo even though it is called "echo" in the ATC domain. In the rest of this paper, the ATCO speeches with echo are regarded as noisy speeches, while their corresponding echo-free counterparts are clean speeches.

Speech enhancement (SE) is applied to eliminate noise interference on speech signals to obtain clean speech with higher intelligibility, which has been successfully applied to many applications, such as hearing aids, voice conversion and ASR system. In the early period, traditional SE methods (Lim and Oppenheim 1978; Boll 1979) usually use heuristic or direct algorithms to achieve denoising tasks. With the development of deep learning techniques, deep neural networks (DNN) are introduced into SE research, which have shown potent noise reduction ability in complex situations.

DNN-based SE models are divided into time-frequency (T-F) and time domain methods. T-F domain methods convert the raw signal to corresponding spectral magnitude as input by using short-time Fourier transform (STFT), which have achieved desired performance on SE task (Hu et al. 2020; Zhang et al. 2020; Chen et al. 2022; Schröter et al. 2022). Although the magnitude represents T-F information of the signal, some limitations are existing in the T-F methods (Wang, He, and Zhu 2021). Both the magnitude and phase information or complex value require high complexity of the model, which remains some challenges.

Time domain methods directly enhance noisy speech from raw waveform because it contains the full information of the signal. Various works have been achieved in convolutional neural networks (CNN), recurrent neural networks and generative adversarial networks (GAN) (Pascual, Bonafonte, and Serra 2017; Chen and Wang 2017; Macartney and Weyde 2018; Defossez, Synnaeve, and Adi 2020; Wang, He, and Zhu 2021; Kim and Seo 2021; Park et al. 2022). The raw waveform has the most local structure (millisecond-level signal) with non-discretization properties, which contain acoustic features such as the speaker's timbre and linguistic patterns that can be obtained in the form of phonemes (Rethage, Pons, and Serra 2018), inspiring us to use time domain method to achieve the denoising task in the ATC domain with the auditory and phonetic demands.

As the front-end processor of the ASR system, SE can provide enhanced signals to reduce the non-robustness of the ASR model to redundant noise. In general, the primary goal of the SE technique is to improve the perceptual quality and

intelligibility of speech for human hearing by modifying the temporal and frequency distributions of speech features. Unfortunately, the perception-oriented SE methods inevitably suffer from an inferior ASR performance due to the different optimization targets between the SE and ASR task. The solution of retraining the ASR model requires extra computational resources and still faces great challenges for its generalizability on different speech corpora.

To address this issue, in this work, a novel recognition-oriented speech enhancement (ROSE) framework is proposed to improve both speech intelligibility and ASR performance, which serves as a plug-and-play tool in ATC scenarios and does not require additional retraining of the ASR model. ROSE is implemented using an encoder-decoder-based U-Net architecture with skip connections in the time domain. To enhance the feature fusion, an attention-based skip-fusion (ABSF) mechanism is applied to mine shared features from encoders using an attention mask (Giri, Isik, and Krishnaswamy 2019), which prevents the model from concatenating the hierarchical features directly. To further enhance the feature spaces, a channel and sequence attention (CSAtt) network is innovatively designed to learn objective-oriented feature weights in dual parallel attention paths by referring to (Lan et al. 2020).

To achieve the recognition-oriented SE model, the multi-objective learning is applied to achieve joint optimization of SE and ASR objectives by introducing the objective-oriented loss function. The details are as follows:

1. The SE is to generate similar T-F features for the noisy speeches by referring to their clean counterparts. The mean absolute error (MAE) loss in the time domain and log-scale STFT-magnitude loss (Arik, Jun, and Damos 2019) in the frequency domain serve as the optimization targets for the SE task.
2. The enhanced output of the SE model for noisy signals only obtains desired performance by generating similar ASR-related features to that of clean signals. To this end, the well-designed algorithms for handcrafted feature engineering, such as spectrogram, Mel-frequency cepstral coefficients (MFCC), etc., inspire us to construct the optimization targets to retain the ASR performance for the SE output based on Fourier-based features.

In summary, the main contributions are as follows:

- An end-to-end deep architecture ROSE is proposed to achieve the SE task of the ATC domain, which addresses the radio speech echo and achieves the desired accuracy without retraining the existing ASR model.
- Multi-objective learning is applied to learn the common representations across the two optimization objectives to achieve the recognition-oriented SE model by introducing the T-F loss of the SE task and Fourier-based loss of the ASR task.
- An ABSF block is applied to achieve feature fusion using an attention mask. A CSAtt block is designed to learn informative features and suppress disturbance factors.
- The experiment results show that ROSE outperforms other state-of-the-art (SOTA) models on both real-world

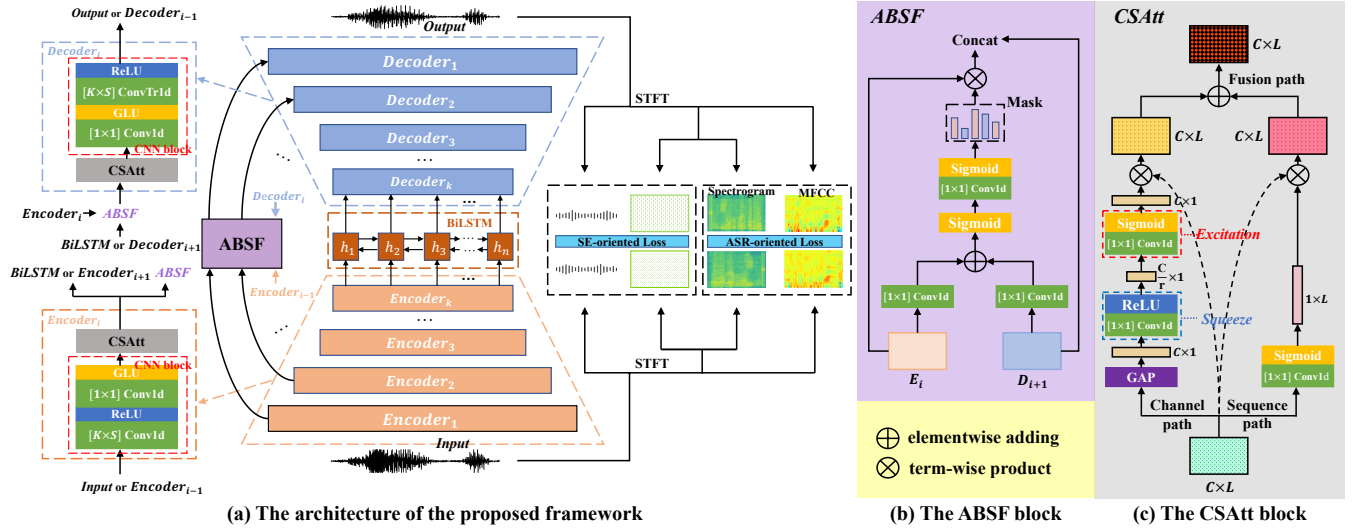


Figure 2: Overall network architecture of ROSE.

ATC corpus and the public open-source datasets for SE and ASR tasks.

ROSE

As shown in Figure 2 (a), the proposed framework is implemented using an end-to-end deep architecture, stacking multiple encoder and decoder layers with U-Net skip connections, in which the index of the decoder layer is the same as that of the corresponding encoder layer. The bidirectional long short-term memory (LSTM) is designed to capture the temporal dependencies among the frames and mine the correlations of signals in the past and future dimensions.

The basic encoder block is comprised of sequential CNN blocks ([strided 1d-convolution (Conv1d), rectified linear unit (ReLU), 1×1 Conv1d, gated linear unit (GLU)]) and CSAtt blocks. To formulate a U-Net shape, the basic decoder block applies an architecture similar to the encoder block, but with a different stacking order, i.e. (1×1 Conv1d, GLU, transposed 1d-convolution (ConvTr1d), ReLU]).

Attention-based Skip-fusion

In general, skip-connection is to transfer shallow encoder features into decoder modules to formulate robust features. However, current practices fuse the encoder and decoder features by addition and concatenation operations with the same weight, which may not be optimal for complex tasks. In this study, the ABSF mechanism is designed to optimize the learned features, in which the gate block is to extract involved correlations from encoded features by multiplying them with an attention mask.

As shown in Figure 2 (b), let the learned feature of the i th encoder layer be E_i , and the learned feature of the $i + 1$ th decoder layer be D_{i+1} . As shown in Equation 1, the convolution operation is applied to the above two feature maps, and the concatenation operation is performed to initialize the

fusion attention coefficient matrix B_i .

$$B_i = \sigma \left(\psi_C^{[1 \times 1]} (E_i) \oplus \psi_C^{[1 \times 1]} (D_{i+1}) \right) \quad (1)$$

where $\psi_C^{[K \times S]}$ are convolution operations with kernel size K and stride S of C filters, \oplus denotes the elementwise adding operation and σ denotes the sigmoid activation. Note that the output feature dimension of the fusion module is the same as that of the input.

Based on the B_i , an attention mask A_i is generated by the convolution network and the selected activation. Finally, the output feature X_i is generated by Equation 2, in which \otimes denotes term-wise product operation.

$$A_i = \sigma \left(\psi_C^{[1 \times 1]} (B_i) \right) \quad X_i = D_{i+1} \oplus (E_i \otimes A_i) \quad (2)$$

The Channel and Sequence Attention

Facing the temporal shift of the speech echo, the transitions between neighbor phonemes are overlapped to cause disordered representations, further impacting the ASR performance. In this work, a dual-attention module is proposed to recalibrate the learned features in a parallel manner, which assigns task-oriented weights on both channel and sequence dimensions, i.e., CSAtt. The proposed module achieves dual attention, which is illustrated as follows:

Channel Path. This path aims to reinforce the model to perceive informative feature channels using the attention mechanism. Considering the fact that the noise and spoken words are distributed in different frequencies of the speech features, channel attention is desired to emphasize the features with higher weights for spoken words and suppress features with lower weights for the noise.

Sequence Path. This path is to guide the model to focus on selective frames by employing higher attention weights. Specifically, the trainable attention module focuses on the marginal frames to remove echo features to support the SE

task and also highlights the central frames of each phoneme to advance the ASR task.

Fusion path. This path is to fuse features learned from channel and sequence paths and feeds them into subsequent modules.

The global average pooling (GAP) operation is applied to generate the sample-related initial weights based on the input feature map. As shown in Figure 2 (c), let the input feature map be $X \in \mathbb{R}^{C \times L}$, where C is the number of channels, L is the length of the sequence dimension. The GAP operation is applied to generate the sample-related initial weights based on the input feature map along the channel dimension. The squeeze-and-excitation attention is to obtain the channel attention weights W_C , as shown below:

$$BX = \delta \left(\psi_{\frac{C}{r}}^{[1 \times 1]}(GAP(X)) \right), BX \in \mathbb{R}^{\frac{C}{r} \times 1} \quad (3)$$

$$W_C = \sigma \left(\psi_C^{[1 \times 1]}(BX) \right), W_C \in \mathbb{R}^{C \times 1} \quad (4)$$

where Equation 3 and 4 denote the channel squeeze and excitation operations, respectively. r is a hyper-parameter to indicate the squeezed degree. δ denotes the ReLU activation. Finally, the output feature of the channel attention X_C is obtained by the following rules:

$$X_C = X \otimes W_C, X_C \in \mathbb{R}^{C \times L} \quad (5)$$

Similarly, the sequence attention weight W_L is obtained by using Conv1d of 1 filter to convolve the input feature X with the activation function. The sequence-attentive feature X_L is obtained by Equation 7:

$$W_L = \sigma \left(\psi_1^{[1 \times 1]}(X) \right), W_L \in \mathbb{R}^{1 \times L} \quad (6)$$

$$X_L = X \otimes W_L, X_L \in \mathbb{R}^{C \times L} \quad (7)$$

Finally, The fused features of the CSAtt block are achieved as below:

$$X_{CSAtt} = X_C \oplus X_L, X_{CSAtt} \in \mathbb{R}^{C \times L} \quad (8)$$

Multi-objective Loss Function

As illustrated before, the proposed model is optimized by multi-objective learning to enhance speech quality and ASR-required features. The MAE loss in the time domain and log-scale STFT-magnitude loss in the frequency domain serve as the optimization targets for the SE task.

Given s and \tilde{s} be the clean and denoised speech signal respectively, the loss function of the SE task L_{SE} is obtained using the following rules:

$$L_{MAE} = \|s - \tilde{s}\|_1 \quad (9)$$

$$L_{MAG} = \|\log |STFT(s; \theta)| - \log |STFT(\tilde{s}; \theta)|\|_F \quad (10)$$

$$L_{SE} = L_{MAE} + L_{MAG} \quad (11)$$

where $\|\cdot\|_1$ and $\|\cdot\|_F$ denote the L_1 and Frobenius norm, respectively. $|STFT(*)|$ denotes the magnitude of signal processed through STFT. θ denotes the STFT parameters (FFT bins, hop sizes, window lengths).

For the ASR task, the spectral convergence (SC) loss is regarded as the optimization target to achieve ASR-required

features. Considering that the common ASR features are based on the STFT operation, such as spectrogram and MFCC. According to (Yamamoto, Song, and Kim 2020), the SC loss can be defined as follows:

$$f(D; \theta) = \|D(s; \theta) - D(\tilde{s}; \theta)\|_F / \|D(s; \theta)\|_F \quad (12)$$

where D denotes the handcrafted features of the speech signal. In this work, spectrogram and MFCC features are selected to implement ASR task L_{ASR} , as shown below:

$$L_{Spec} = f(Spectrogram; \theta) \quad L_{MFCC} = f(MFCC; \theta) \quad (13)$$

$$L_{ASR} = L_{Spec} + L_{MFCC} \quad (14)$$

Finally, the total loss is formulated to achieve the multi-objective training with two hyper-parameters as below:

$$L = \lambda_1 L_{SE} + \lambda_2 L_{ASR} \quad (15)$$

Experiments

Dataset

A real-world dataset is collected from an industrial ATC system. Detailed descriptions of dataset are shown in Appendix. As mentioned above, the ATCO speech with echo is defined as noisy and corresponding echo-free speech is defined as clean. All samples are multilingual with various ATC instructions and are sampled at 8 kHz. The text labels are annotated for the test set to evaluate the ASR performance.

Experimental Configurations

In the ROSE, the depth of both the encoder and decoder are 5 and the hidden dimension of each layer is $H = 48$. For the CNN block of encoder/decoder, Conv1d or ConvTr1d is configured with kernel size $K = 8$ and stride $S = 4$. For the CSAtt block, r is set to 2 for squeezing the feature channels. Two bidirectional LSTM layers with 768 neurons are designed to capture the sequential dependencies. For the STFT parameters, FFT bins are 512, hop sizes are 100, and window lengths are 400. The dimension of MFCC is set to 13. The λ_i for the loss function in Equation 15 is set to 1. The Adam optimizer is applied to optimize the proposed framework with an initial learning rate of 3e-4 and 0.999 decay. All samples are upsampled from 8 kHz to 16 kHz and clipped to 4 seconds long. The batch size is set to 64 during the model training.

To confirm the effectiveness and efficiency of the proposed model on ASR performance, the test set is evaluated using a Deepspeech 2 (DS2) (Amodei et al. 2016) based model trained on the ATCSpeech corpus (Yang et al. 2020).

Baseline Methods and Evaluation Metrics

In this work, several open-source SOTA baselines with the different domains are selected to validate the proposed model, which are classified as follows: 1) *time domain*: Wiener (Lim and Oppenheim 1978), SEGAN (Pascual, Bonafonte, and Serra 2017), DEMUCS (Defossez, Synnaeve, and Adi 2020) and SE-Conformer (Kim and Seo

Score	Descriptions
1	Unable to understand spoken words
2	Some spoken words can be understood, but cannot be organized as ATC instructions
3	Can understand most spoken words of the ATC instructions
4	Can understand ATC instructions clearly and repeat the spoken words

Table 1: Details of the ATC-related subjective measure.

2021), 2) *T-F domain*: CRN (Tan and Wang 2019), DCCRN-E (Hu et al. 2020), MetricGAN+ (Fu et al. 2021) and Full-SubNet+ (Chen et al. 2022). All of those methods are conducted on the official configurations.

For the metrics of the SE task, we compute the following five typical objective measures on the test set, i.e., mean opinion score (MOS) prediction of the *i*) signal distortion attending only to the speech signal (CSIG), *ii*) intrusiveness of background noise (CBAK), *iii*) the overall effect (COVL) (from 1 to 5) (Hu and Loizou 2008), perceptual evaluation of speech quality (PESQ) (from -0.5 to 4.5) (Recommendation 2001), short-time objective intelligibility (STOI) (from 0 to 100) (Taal et al. 2011).

For the subjective evaluation, we randomly sample 10 utterances with complete ATC instructions and each one was scored by 45 ATC experts along two facets: 1) a relevant subjective MOS study is recommended in ITU-T P.835 (recommendation 2003), including level of signal distortion (SIG), intrusiveness of background noise (BAK), and overall quality (OVL). 2) an ATC-related subjective measure is proposed to rate the ATC instructions recognition (AIR) and detailed descriptions are shown in Table 1. For all the above metrics, a larger score indicates a higher speech quality.

For the metric of the ASR task, the label error rate (LER) based on the minimum basic unit of languages is applied to evaluate the ASR performance.

Results and Discussions

Performance Evaluation

The experimental results for the performance comparison are shown in Table 2 (group A). The following conclusions can be obtained from the experimental results:

(1) From experiments A1 and A2, the traditional SE method (Wiener) fails to suppress the speech echo, and even causes extra noise to deteriorate the quality of the original speeches. The results also indicate that the speech echo is a dedicated phenomenon in the ATC domain, which cannot be addressed by the traditional denoising method.

(2) According to experiments A3 and A7, although the GAN-based method improves the objective and subjective metrics of the noisy speech, it deteriorates the ASR accuracy due to the generation mechanism for pseudo-speech by learning the data distribution of clean signals. The main purpose is to satisfy the auditory requirements of the speech quality but fails to enclose ASR-required features to achieve desired recognition accuracy.

(3) According to the supervised-based DNN models, the time-domain methods (A5, A8 and A10) are generally superior to the T-F domain methods (A4, A6, A7 and A9) in terms of objective metrics, and have a significant advantage in ASR performance. The results show that the T-F methods use T-F representatives operated by STFT as input, which inevitably discards potential acoustic and linguistic features, leading to undesirable results.

(4) By focusing on the ASR performance, all the comparative baselines suffer inferior LER compared to the noisy speeches (only marginal improvements obtained by the A8) since they are SE-oriented approaches to improve the auditory quality. The metrics of AIR indicate that improving the clarity and intelligibility of speech can indeed improve the rater’s ability to understand ATC instructions.

Among all comparative methods, the proposed model ROSE achieves the best performance for both the SE and ASR tasks.

Ablation Study

To validate the effectiveness of the multi-objective learning mechanism, ablation experiments are conducted by combining different loss functions in the proposed model (A3). As shown in Table 2 (group B), by incorporating the SC loss into ASR-required features learning, the ASR performance can be considerably enhanced by the multi-objective framework without any model retraining, which validates the core motivation of this work. Compared to the spectrogram features, the MFCC-based SC loss achieves better improvement since it is a more sophisticated handcrafted feature (B1 vs. B2). The best performance is reached by combining the two SC losses, from 4.29% to 3.50% (A10 vs. B3). Except for the ASR performance, the proposed model also harvests higher SE performance. The results can be attributed that the multi-objective loss learns the common representations across the two optimization objectives thanks to its powerful ability on feature learning.

To validate the ability of the proposed attention modules, ablation experiments are conducted by combining different attention blocks in the single-objective model (B3). As can be seen from Table 2 (group C), both ABSF and CSAtt blocks can enhance the model performance in terms of both the SE- and ASR-related metrics. Specifically, compared to the ABSF block, the CSAtt can achieve higher performance improvement by optimizing the learned features, where objective metrics are improved by about 0.23 on average and LER is decreased by 0.05% (C1 vs. C2). To be specific, the attention module focuses on informative feature channels to suppress noise interference, while highlighting selective frames to fit the data distribution between features and text labels. Finally, the proposed model can achieve the best performance by combining the two attention blocks (B3 vs. C3), which validates the proposed model architecture.

Experiments on public datasets

Experiments for the SE Several representative SOTA models with different inputs are selected to compare with ROSE on Voice Bank + DEMAND dataset (Valentini-Botinhao et al. 2016). Specifically, four types of input are

Exp.	Model	pred. CSIG \uparrow	pred. CBAK \uparrow	pred. COVL \uparrow	PESQ \uparrow	STOI \uparrow (%)	MOS SIG \uparrow	MOS BAK \uparrow	MOS OVL \uparrow	AIR \uparrow	LER \downarrow (%)
A1	Noisy	3.28	1.81	2.48	1.80	56.39	3.42	2.84	2.91	3.4	4.66
A2	Wiener (T)	2.17	1.41	1.66	1.49	54.20	2.78	2.13	2.26	3.1	10.62
A3	SEGAN (T)	3.56	2.55	2.79	2.12	69.90	3.47	2.85	2.93	3.4	9.74
A4	CRN (T-F)	3.57	2.51	2.89	2.33	70.91	3.54	2.78	2.94	3.5	7.97
A5	DEMUCS (T)	4.25	2.95	3.45	2.66	80.34	3.89	3.21	3.15	3.6	4.72
A6	DCCRN-E (T-F)	3.76	2.69	3.07	2.45	70.64	3.62	3.03	2.95	3.5	8.46
A7	MetricGAN+ (T-F)	4.13	3.12	3.41	2.97	72.19	3.78	3.19	3.02	3.5	7.98
A8	SE-Conformer (T)	4.40	3.15	3.69	3.02	81.23	3.83	3.21	3.13	3.7	4.28
A9	FullSubNet+ (T-F)	4.12	3.00	3.45	2.82	74.85	3.82	3.18	3.10	3.6	5.35
A10	ROSE (Ours) (T)	4.58	3.22	3.85	3.09	83.90	3.98	3.24	3.15	3.8	3.50
B1	A10 w/o L_{Spec}	4.42	3.08	3.64	2.85	83.04	-	-	-	-	4.00
B2	A10 w/o L_{MFCC}	4.40	3.04	3.64	2.88	82.65	-	-	-	-	4.08
B3	A10 w/o L_{ASR}	4.33	3.01	3.53	2.71	82.15	-	-	-	-	4.29
C1	B3 w/o ABSF	4.27	2.94	3.46	2.66	81.60	-	-	-	-	4.31
C2	B3 w/o CSAAtt	4.15	2.84	3.33	2.51	79.79	-	-	-	-	4.36
C3	B3 w/o <i>attn.</i>	4.04	2.76	3.21	2.39	79.37	-	-	-	-	4.40

Table 2: Experiments for different methods and ablation studies on ATC corpus. The LER of clean signal is 2.25.

Model	Input	CSIG \uparrow	CBAK \uparrow	COVL \uparrow	PESQ \uparrow	STOI (%) \uparrow
Noisy	-	3.35	2.44	2.63	1.97	92
Wiener (Lim and Oppenheim 1978)	Waveform	3.23	2.68	2.67	2.22	93
SEGAN (Pascual, Bonafonte, and Serra 2017)	Waveform	3.48	2.94	2.80	2.16	-
CRN (Tan and Wang 2019)	Magnitude	3.59	3.11	2.71	2.48	93
MetricGAN (Fu et al. 2019)	Magnitude	3.99	3.18	3.42	2.86	-
CRGAN (Zhang et al. 2020)	Magnitude	4.16	3.24	3.54	2.92	94
DEMUCS (Defossez, Synnaeve, and Adi 2020)	Waveform	4.31	3.40	3.63	3.07	95
DCCRN-E (Hu et al. 2020)	RI	3.74	3.13	2.75	2.54	94
MetricGAN+ (Fu et al. 2021)	Magnitude	4.14	3.16	3.64	3.15	-
TSTNN (Wang, He, and Zhu 2021)	Waveform	4.17	3.53	3.49	2.96	95
SE-Conformer (Kim and Seo 2021)	Waveform	4.45	3.55	3.82	3.13	95
CTS-Net (Li et al. 2021)	RI+Magnitude	4.25	3.46	3.59	2.92	-
FullSubNet+ (Chen et al. 2022)	RI+Magnitude	3.86	3.42	3.57	2.88	94
GaGNet (Li et al. 2022)	RI+Magnitude	4.26	3.45	3.59	2.94	95
DeepFilterNet2 (Schröter et al. 2022)	RI+Magnitude	4.30	3.40	3.70	3.08	94
ROSE (Ours)	Waveform	4.47	3.56	3.72	3.01	95

Table 3: SE results on Voice Bank + DEMAND dataset, “-” denotes the result is not provided in the associated papers.

classified as: 1) *Waveform*, 2) *Magnitude*, 3) *Real-imaginary (RI)* and 4) *RI + Magnitude*.

The experimental results are reported in Table 3. Although ROSE does not achieve the best performance on COVL and ROSE, it still outperforms comparative SOTA models in terms of other metrics. Inside the MetricGAN (+) methods, due to the PESQ-oriented optimization target involved in the training procedure, the models have achieved cliff-like superiorities on PESQ, while other metrics are inferior. This result shows that the objective-oriented loss function can improve task-oriented feature learning. In addition, it can also be found that the traditional method (Wiener) can achieve better performance on the public dataset with artificial noise models, which also supports the

research specificities of the ATC speech corpus with real-world noise and speech echo phenomenon.

Experiments for the ASR To validate the ASR performance of ROSE on the public dataset, according to the mixed type of signals, two datasets based on test-clean samples in the Librispeech dataset (Panayotov et al. 2015) are artificially synthesized, which are additive noise and simulative echo datasets. Specifically, the mixed noisy samples of the additive noise dataset are formed by mixing each utterance of test-clean samples with the noises from the test set of DNS benchmark (Reddy et al. 2020) with 4 SNR levels (-3, 0, 3, and 6 dB).

To simulate as much as possible the speech echo in the ATC domain, each utterance of test-clean samples is

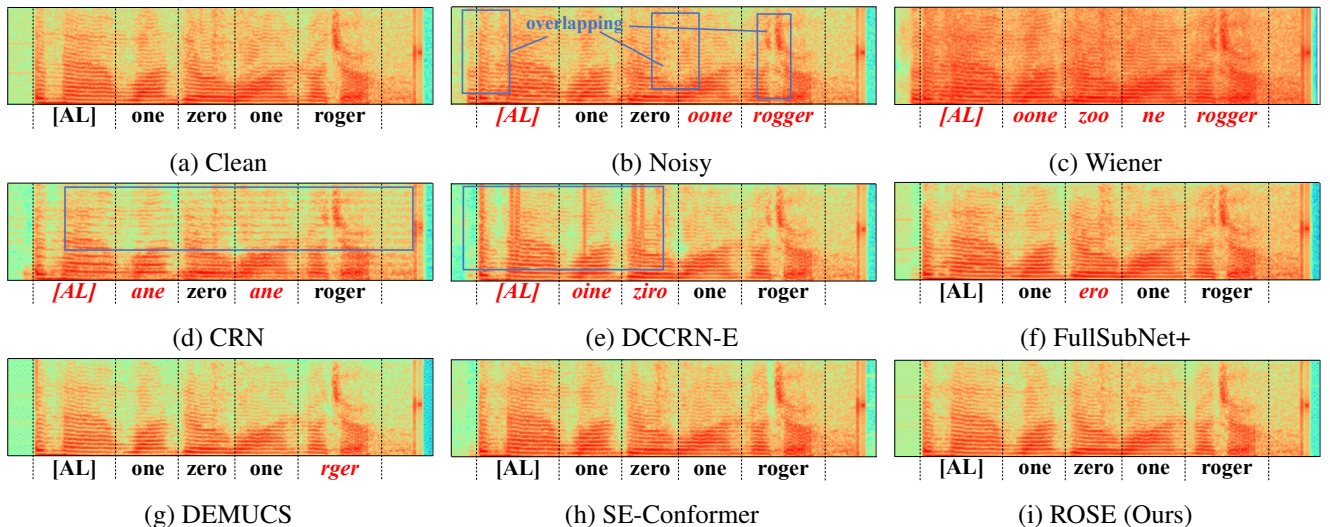


Figure 3: Visualization for the Spectrograms and ASR results.

Model	Input	a LER(%) ↓	e LER(%) ↓
Mixed	-	33.36	42.72
CRN	Magnitude	35.68	38.23
SE-Conformer	Waveform	21.43	31.10
DCCRN-E	RI	26.69	33.67
ROSE (Ours)	Waveform	12.75	22.31
<i>w/o</i> L_{ASR}	Waveform	19.12	29.44
<i>w/o</i> <i>attn.</i>	Waveform	17.86	26.56
test-clean	-		9.97

Table 4: ASR results on two artificial datasets. "a" denotes additive noise, "e" denotes simulative echo.

copied twice to reproduce the ATC communication process. The samples are mixed with 30dB and 10dB Gaussian white noises to simulate the sent and more complex received speeches (mentioned in Figure 1) respectively. Finally, the mixed noisy samples of the simulative echo dataset are formed by overlapping the above two samples with a random temporal delay between 10 and 200 milliseconds and clipped to ensure the temporal alignment with test-clean samples. Note that the test-clean samples are treated as echo-free speeches for comparison with the additive noise dataset.

Several models with different inputs trained on Voice Bank + DEMAND dataset are selected to enhance blind artificial datasets. Acoustic model based on DS2 retrained from scratch on Librispeech dataset is used to validate the ASR performance.

The experimental results are reported in Table 4. Speech is a continuous sequence, in which there are strong temporal correlations between adjacent frames. Compared to additive noise, signal overlapping severely degrades the discriminability of text-related features, leading to collapsed representatives. Compared with waveform, taking T-F features (Magnitude or RI) as input will inevitably lose some

potential linguistic features due to additional operation (e.g. STFT), resulting in inferior ASR performance (The a LER of CRN is even worse than that of Mixed). The proposed attention modules and multi-objective mechanism achieve improvements on both two datasets, where the model combined with ASR-oriented target achieves significant results (a LER from 19.12% to 12.75% and e LER from 29.44% to 22.31%, respectively).

Visualization

To better demonstrate the performance of each model on SE and ASR tasks, we select a pure English example from the test set of the ATC corpus (the selected speech text ground-truth is: *[AL] one zero one roger*, in which [AL] refers to the airline) and draw the spectrums in different cases.

As shown in Figure 3, compared with the clean spectrogram (a), the noisy spectrogram (b) has obvious overlapping phenomena, resulting in blurred gaps between English word pronunciations. Wiener (c) not only fails to effectively remove noise components but also brings redundant signals to speech, resulting in inferior ASR performance.

There are some defects in the selected T-F domain methods. The high-frequency area of CRN (d) shows sparseness leading to collapsed features. The sequence of DCCRN-E (e) has unexpected mutational signals, which further affect the stationarity of the speech. On the contrary, the time domain methods achieve superior performance, especially the ROSE (i) obtains the result closest to clean (a).

Other relevant visualizations are shown in Appendix.

Conclusions

In this study, a recognition-oriented speech enhancement model (ROSE) based on multi-objective learning is proposed to achieve the SE task of the ATC domain, while improving the ASR performance without model retraining. Specifically, The ABSF and CSAtt blocks highlight informative information and suppress redundant factors, enhanc-

ing the ability of the model to learn objective-related features. The multi-objective learning acquires the common representations across the two optimization objectives by combining the task-oriented loss function, achieving mutual promotion of SE and ASR tasks performance. The experiment results show that the proposed framework can not only achieve the desired performance on the ATC corpus, but can be generalized to the public open-source datasets.

References

- Amodei, D.; Ananthanarayanan, S.; Anubhai, R.; Bai, J.; Battenberg, E.; Case, C.; Casper, J.; Catanzaro, B.; Cheng, Q.; Chen, G.; Chen, J.; Chen, J.; Chen, Z.; Chrzanowski, M.; Coates, A.; Diamos, G.; Ding, K.; Du, N.; Elsen, E.; Engel, J.; Fang, W.; Fan, L.; Fougner, C.; Gao, L.; Gong, C.; Hannun, A.; Han, T.; Johannes, L. V.; Jiang, B.; Ju, C.; Jun, B.; LeGresley, P.; Lin, L.; Liu, J.; Liu, Y.; Li, W.; Li, X.; Ma, D.; Narang, S.; Ng, A.; Ozair, S.; Peng, Y.; Prenger, R.; Qian, S.; Quan, Z.; Raiman, J.; Rao, V.; Satheesh, S.; Seetapun, D.; Sengupta, S.; Srinet, K.; Sriram, A.; Tang, H.; Tang, L.; Wang, C.; Wang, J.; Wang, K.; Wang, Y.; Wang, Z.; Wang, Z.; Wu, S.; Wei, L.; Xiao, B.; Xie, W.; Xie, Y.; Yogatama, D.; Yuan, B.; Zhan, J.; and Zhu, Z. 2016. Deep Speech 2: End-to-End Speech Recognition in English and Mandarin. In *33rd International Conference on Machine Learning*, volume 48, 173–182. JMLR-JOURNAL MACHINE LEARNING RESEARCH.
- Arik, S. O.; Jun, H.; and Diamos, G. 2019. Fast Spectrogram Inversion Using Multi-Head Convolutional Neural Networks. *IEEE Signal Processing Letters*, 26(1): 94–98.
- Badrinath, S.; and Balakrishnan, H. 2022. Automatic Speech Recognition for Air Traffic Control Communications. *Transportation Research Record*, 2676(1): 798–810.
- Boll, S. F. 1979. Suppression of acoustic noise in speech using spectral subtraction. *IEEE Transactions on Acoustics, Speech, and Signal Processing*, 27(2): 113–120.
- Chen, J.; and Wang, D. 2017. Long short-term memory for speaker generalization in supervised speech separation. *Journal of the Acoustical Society of America*, 141(6): 4705–4714.
- Chen, J.; Wang, Z.; Tuo, D.; Wu, Z.; Kang, S.; and Meng, H. 2022. FullSubNet+: Channel Attention FullSubNet with Complex Spectrograms for Speech Enhancement. In *ICASSP 2022-2022 IEEE International Conference on Acoustics, Speech and Signal Processing (ICASSP)*, 7857–7861. IEEE.
- Defossez, A.; Synnaeve, G.; and Adi, Y. 2020. Real Time Speech Enhancement in the Waveform Domain. In *Inter-speech Conference*, 3291–3295. ISCA-INT SPEECH COMMUNICATION ASSOC.
- Fu, S.-W.; Liao, C.-F.; Tsao, Y.; and Lin, S.-D. 2019. Metricgan: Generative adversarial networks based black-box metric scores optimization for speech enhancement. In *International Conference on Machine Learning*, 2031–2041. PMLR.
- Fu, S.-W.; Yu, C.; Hsieh, T.-A.; Plantinga, P.; Ravanelli, M.; Lu, X.; and Tsao, Y. 2021. MetricGAN plus : An Improved Version of MetricGAN for Speech Enhancement. In *INTER-SPEECH 2021*, Interspeech, 201–205. Interspeech Conference, Brno, CZECH REPUBLIC, AUG 30-SEP 03, 2021.
- Giri, R.; Isik, U.; and Krishnaswamy, A. 2019. Attention wave-u-net for speech enhancement. In *2019 IEEE Workshop on Applications of Signal Processing to Audio and Acoustics (WASPAA)*, 249–253. ISCA-INT SPEECH COMMUNICATION ASSOC. ISBN 978-1-7281-1123-0.
- Hu, Y.; Liu, Y.; Lv, S.; Xing, M.; Zhang, S.; Fu, Y.; Wu, J.; Zhang, B.; and Xie, L. 2020. DCCRN: Deep Complex Convolution Recurrent Network for Phase-Aware Speech Enhancement. In *INTERSPEECH 2020*, Interspeech, 2472–2476. Interspeech Conference, Shanghai, PEOPLES R CHINA, OCT 25-29, 2020.
- Hu, Y.; and Loizou, P. C. 2008. Evaluation of objective quality measures for speech enhancement. *IEEE Transactions on Audio, Speech and Language Processing*, 16(1): 229–238.
- Kim, E.; and Seo, H. 2021. SE-Conformer: Time-Domain Speech Enhancement Using Conformer. In *Interspeech*, 2736–2740.
- Lan, T.; Lyu, Y.; Ye, W.; Hui, G.; Xu, Z.; and Liu, Q. 2020. Combining multi-perspective attention mechanism with convolutional networks for monaural speech enhancement. *IEEE Access*, 8: 78979–78991.
- Li, A.; Liu, W.; Zheng, C.; Fan, C.; and Li, X. 2021. Two Heads are Better Than One: A Two-Stage Complex Spectral Mapping Approach for Monaural Speech Enhancement. *IEEE-ACM TRANSACTIONS ON AUDIO SPEECH AND LANGUAGE PROCESSING*, 29: 1829–1843.
- Li, A.; Zheng, C.; Zhang, L.; and Li, X. 2022. Glance and gaze: A collaborative learning framework for single-channel speech enhancement. *Applied Acoustics*, 187: 108499.
- Lim, J. S.; and Oppenheim, A. V. 1978. All-pole modeling of degraded speech. *IEEE Transactions on Acoustics, Speech, and Signal Processing*, 26(3): 197–210.
- Lin, Y.; Guo, D.; Zhang, J.; Chen, Z.; and Yang, B. 2021a. A Unified Framework for Multilingual Speech Recognition in Air Traffic Control Systems. *IEEE Transactions on Neural Networks and Learning Systems*, 32(8): 3608–3620.
- Lin, Y.; Li, Q.; Yang, B.; Yan, Z.; Tan, H.; and Chen, Z. 2021b. Improving speech recognition models with small samples for air traffic control systems. *Neurocomputing*, 445: 287–297.
- Lin, Y.; Yang, B.; Guo, D.; and Fan, P. 2021c. Towards multilingual end-to-end speech recognition for air traffic control. *IET Intelligent Transport Systems*, 15(9): 1203–1214.
- Macartney, C.; and Weyde, T. 2018. Improved speech enhancement with the wave-u-net. arXiv:1811.11307.
- Oualil, Y.; Klakow, D.; Szaszak, G.; Srinivasamurthy, A.; Helmke, H.; and Motlicek, P. 2017. A context-aware speech recognition and understanding system for air traffic control domain. In *2017 IEEE Automatic Speech Recognition and Understanding Workshop (ASRU)*, 404–408. IEEE. ISBN 978-1-5090-4788-8.
- Panayotov, V.; Chen, G.; Povey, D.; and Khudanpur, S. 2015. Librispeech: an asr corpus based on public domain audio

- books. In *2015 IEEE international conference on acoustics, speech and signal processing (ICASSP)*, 5206–5210. IEEE.
- Park, H. J.; Kang, B. H.; Shin, W.; Kim, J. S.; and Han, S. W. 2022. Manner: Multi-view attention network for noise erasure. In *ICASSP 2022-2022 IEEE International Conference on Acoustics, Speech and Signal Processing (ICASSP)*, 7842–7846. IEEE.
- Pascual, S.; Bonafonte, A.; and Serra, J. 2017. SEGAN: Speech Enhancement Generative Adversarial Network. In *18th Annual Conference of the International-Speech-Communication-Association (INTERSPEECH 2017)*, 3642–3646. ISCA-INT SPEECH COMMUNICATION ASSOC. ISBN 978-1-5108-4876-4.
- Recommendation, I.-T. 2001. Perceptual evaluation of speech quality (PESQ): An objective method for end-to-end speech quality assessment of narrow-band telephone networks and speech codecs. *Rec. ITU-T P. 862*.
- recommendation, I.-T. 2003. Subjective test methodology for evaluating speech communication systems that include noise suppression algorithm. *ITU-T Rec. P.835*.
- Reddy, C. K.; Gopal, V.; Cutler, R.; Beyrami, E.; Cheng, R.; Dubey, H.; Matushevych, S.; Aichner, R.; Aazami, A.; and Braun, S. 2020. The interspeech 2020 deep noise suppression challenge: Datasets, subjective testing framework, and challenge results. arXiv:2005.13981.
- Rethage, D.; Pons, J.; and Serra, X. 2018. A wavenet for speech denoising. In *2018 IEEE International Conference on Acoustics, Speech and Signal Processing (ICASSP)*, 5069–5073. IEEE.
- Schröter, H.; Escalante-B., A. N.; Rosenkranz, T.; and Maier, A. 2022. DeepFilterNet2: Towards Real-Time Speech Enhancement on Embedded Devices for Full-Band Audio. In *17th International Workshop on Acoustic Signal Enhancement (IWAENC 2022)*.
- Taal, C. H.; Hendriks, R. C.; Heusdens, R.; and Jensen, J. 2011. An Algorithm for Intelligibility Prediction of Time-Frequency Weighted Noisy Speech. *IEEE Transactions on Audio, Speech and Language Processing*, 19(7): 2125–2136.
- Tan, K.; and Wang, D. 2019. Complex spectral mapping with a convolutional recurrent network for monaural speech enhancement. In *ICASSP 2019-2019 IEEE International Conference on Acoustics, Speech and Signal Processing (ICASSP)*, 6865–6869. IEEE.
- Valentini-Botinhao, C.; Wang, X.; Takaki, S.; and Yamagishi, J. 2016. Investigating RNN-based speech enhancement methods for noise-robust Text-to-Speech. In *SSW*, 146–152.
- Wang, K.; He, B.; and Zhu, W.-P. 2021. TSTNN: Two-stage transformer based neural network for speech enhancement in the time domain. In *ICASSP 2021-2021 IEEE International Conference on Acoustics, Speech and Signal Processing (ICASSP)*, 7098–7102. IEEE.
- Yamamoto, R.; Song, E.; and Kim, J.-M. 2020. Parallel WaveGAN: A fast waveform generation model based on generative adversarial networks with multi-resolution spectrogram. In *IEEE International Conference on Acoustics, Speech, and Signal Processing*, 6199–6203. IEEE. ISBN 978-1-5090-6631-5.
- Yang, B.; Tan, X.; Chen, Z.; Wang, B.; Ruan, M.; Li, D.; Yang, Z.; Wu, X.; and Lin, Y. 2020. ATCSpeech: A Multilingual Pilot-Controller Speech Corpus from Real Air Traffic Control Environment. In *Interspeech Conference*, 399–403.
- Zhang, Z.; Deng, C.; Shen, Y.; Williamson, D. S.; Sha, Y.; Zhang, Y.; Song, H.; and Li, X. 2020. On Loss Functions and Recurrency Training for GAN-based Speech Enhancement Systems. In *INTERSPEECH 2020*, Interspeech, 3266–3270.